ISSN Print: 2394-7500
ISSN Online: 2394-5869
Impact Factor: 5.2
IJAR 2016; 2(12): 665-668
www.allresearchjournal.com
Received: 09-10-2016
Accepted: 10-11-2016

E Nagaraja
Department of Physics, Kuvempu University, Shankaraghatta, Karnataka, India

AS Jagadisha
Department of Physics, Kuvempu University, Shankaraghatta, Karnataka, India

Thejas Urs G
Center for Materials Science, Vijnana Bhavan, University of Mysore, Manasagangotri Campus, Mysore, India

HS Jayanna
Department of Physics, Kuvempu University, Shankaraghatta, Karnataka, India

Correspondence
H S Jayanna
Department of Physics, Kuvempu University, Shankaraghatta, Karnataka, India

Effect of gamma irradiation on structural and DC electrical properties of $CdFe_2O_4$ ferrite

E Nagaraja, AS Jagadisha, Thejas Urs G and HS Jayanna

Abstract
$CdFe_2O_4$ ferrite was prepared by ceramic technique. Structural properties were determined by X-ray diffraction. Surface morphological and elemental compositions of the prepared samples were studied by high resolution scanning electron microscopy and energy dispersive spectroscopy (EDS). The prepared samples were irradiated to high energy gamma radiation of ^{60}Co source with a dose rate of 6.972 kGy/hr to different doses of 300kGy and 500kGy. The XRD spectra were obtained for the irradiated samples and compared with that of the pristine samples to study the changes in the structure. The obtained results showed that the crystallite size decreases and lattice strain increases with increase of radiation dose. The DC electrical conductivity at room temperature studies showed the increase of conductivity and decrease of activation energies with radiation dose.

Keywords: Gamma irradiation, cadmium ferrite, electrical conductivity

1. Introduction
India The structural, electrical and magnetic properties of cadmium ferrite sample, prepared by different methods, are reported by several researchers. Its applications also include gas sensors [1], antibacterial activity [9] and photo catalysts [2]. Cadmium ferrite ($CdFe_2O_4$) has a normal spinel structure AB_2O_4 in which eight tetrahedral (A-sites) sites contain divalent and sixteen octahedral (B-sites) sites contain trivalent metal ions $(Cd^{2+})_t$ $[Fe^{3+}$ $Fe^{3+}]_oO_4^{2-}$. Cadmium is antiferromagnetic and show n-type conduction.
Irradiation of ferrites using fast neutrons, high energy ions and γ-rays is important, because the radiant energy can produce crystallographic defects and cause changes in electrical or magnetic properties of ferrites. In the present work we have investigated the effect γ–irradiation on structural and d c electrical properties of $CdFe_2O_4$ ferrite.

2. Experimental
The AR grade CdO and Fe_2O_3 are mixed in the stoichiometric ratio. The mixture is ground to a very fine powder using an agate mortar for 2 hours and pre-sintered at 800^0C temperature for 8 hours. Then again the compositions are ground for 4 hours and pressed in the form of tablets. Final sintering was done at 1200^0C for 12 hours and then samples are allowed to cool to room temperature. The formation of spinel phase and crystal structure is confirmed by X-ray diffraction using Cu-K_α radiation of wavelength $1.5405A^0$ over the 2θ range of 10^0-60^0 with a scanning rate of 2^0/min. The samples are irradiated with the energetic gamma radiation using ^{60}Co source with dose rate of 6.972kGy/hr. The radiation source ^{60}Co is located at Centre for Application of Radioisotopes and Radiation Technology (CARRT), Mangalore University, Mangalore, India. Micro structural analysis of the prepared samples is carried out by Scanning Electron Microscopy (SEM). EDAX is used to determine the quantities of cadmium and Iron in the prepared samples.
The DC electrical conductivity is measured from room temperature up to about 600 K by inserting the tablet samples between two silver electrodes, using the two-probe method. The investigated samples are polished and coated with silver paste at both surfaces to have good electrical contact.

The conductivity of the sample (σ) is calculated using the relation,

$$\sigma = \frac{d}{RA} \qquad ...1$$

Where, R the resistance, A the cross-section area and d the thickness of the sample.

3. Results and discussions

3.1 XRD measurement

The room temperature X-ray diffraction patterns of all the samples of $CdFe_2O_4$ ferrite, before and after gamma irradiation are shown in Fig. 1. X-ray diffraction pattern shows all the allowed reflection lines corresponding to cubic spinel phase.

The average crystallite size of the prepared ferrite samples are determined from the full width half maximum (FWHM) of most intense peak (311) using Debye-Scherrer equation.

$$D = \frac{k\lambda}{\beta Cos\theta} \qquad ...2$$

Where, k Scherrer factor (0.9), λ wavelength of X-ray ($1.5046A^0$), β angular line width at half maximum intensity and θ is the Bragg angle of actual peak.

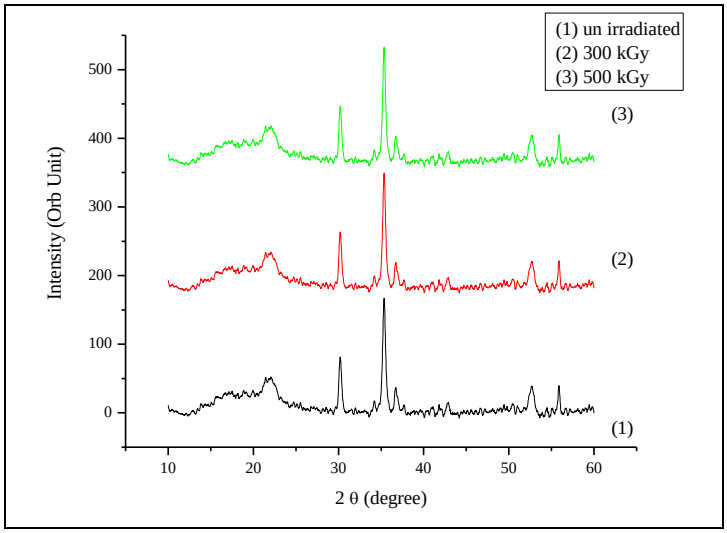

Fig 1: XRD pattern of un-irradiated and irradiated samples of $CdFe_2O_4$ferrite.

The crystallite size (D) and lattice strain of the investigated samples are listed in table 1. D lies in the range of 7 to 35 nm. From the data it can be observed that, crystallite size decreases and lattice strain increases with radiation dose. This can be attributed to strong effect of ionizing γ-radiation on the structure of the ferrite samples. Similar results for the rare earth ferrites are reported by E. Ateia, (2006) [3].

Table 1: Variation of crystallite size and lattice strain before and after irradiation.

Dose in kGy	Crystallite size in nm (D)	Lattice strain
0	35.43	0.06%
300	12.66	0.36%
500	7.94	0.92%

After γ-irradiation the peak positions are slightly shifted to higher 2θ values (Fig.1). This may be due to creation of lattice vacancies resulting in structure distortion and deviation from the spinel cubic structure. It may also be due to irradiation induced the compressive strain (Table 1) and generated some disorder in the lattice structure [4]. Similar behavior is reported in the case of high energy ion interactions [5- 8].

After γ-irradiation width of the major peaks are broadened (Fig.1) due to decrease of the crystallite size.

3.2 SEM Studies

Scanning electron microscopy analysis was performed in order to investigate the microstructure and morphology of irradiated and un-irradiated ferrite samples using FEIXL 40 SIRION FEG digital scanning microscope.

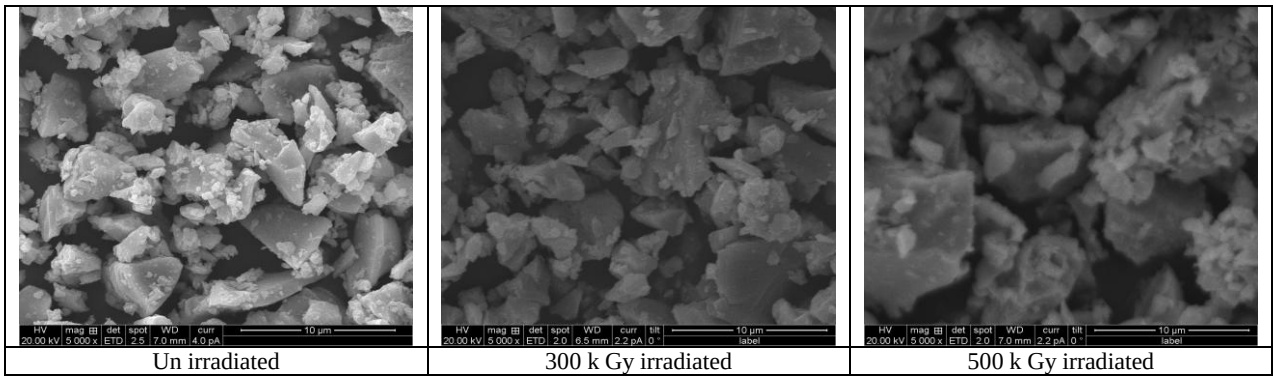

Un irradiated	300 k Gy irradiated	500 k Gy irradiated

Fig 2: SEM morphology of $CdFe_2O_4$ ferrite samples.

The images show that the particles have an almost homogeneous distribution, and some of them are in an agglomerated form. The particles are observed as uniform grains (in different SEM images) confirming the crystalline structure of $CdFe_2O_4$ ferrites which are detected by XRD studies.

3.3 Elemental analysis by EDS

The elemental analysis of the $CdFe_2O_4$ ferrite is done by the Energy Dispersive Spectrometer (EDS). The elemental percentage (%) and atomic percentage (%) of different elements in the samples are shown in the Table 2. The EDS pattern of the sample is shown in Figure 3 which indicates the elemental and atomic composition of the sample.

Table 2: EDS analysis of elemental percentage and atomic percentage of prepared sample.

Element	Wt (%)	At (%)
O	9.67	31.95
Cd	36.59	17.20
Fe	53.74	50.85

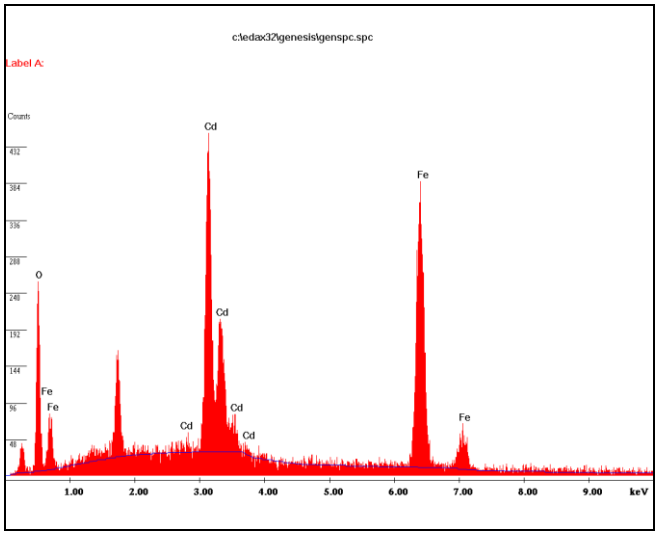

Fig 3: EDS pattern of prepared the prepared sample.

3.4 D C electrical conductivity

Figure 4 shows the variation of DC conductivity at room temperature with radiation dose. Conductivity is increased with γ-irradiation dose. Earlier it is reported that the amount of Fe^{2+} ions on B-sites greatly affects the conductivity [10, 11]. The electrical conductivity is directly proportional to the amount of Fe^{2+} ions. The increase of Fe^{2+} ions concentration enhances the hopping probability of the electrons between Fe^{2+} and Fe^{3+} ions in B-sites, [12].

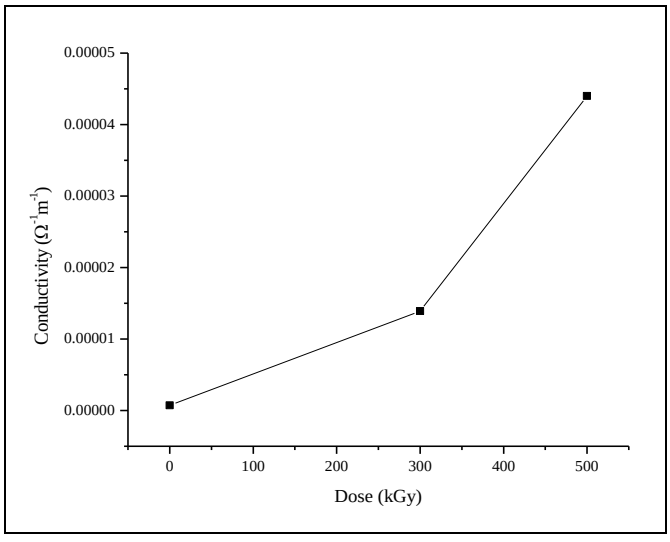

Fig 4: Variation of D C conductivity at room temperature with dose.

The increase of conductivity with γ-irradiation could be attributed to the increase in the ratio of Fe^{2+}/Fe^{3+} on B-sites. Similar behavior is reported by several authors for different ferrites [3, 13, 14, 15].

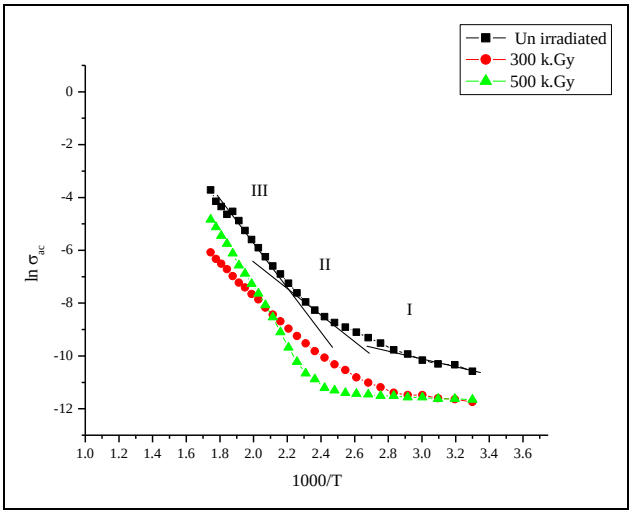

Fig 5: Variation of D C conductivity with temperature.

It is evident from the graphs (Fig.5) that the electrical conductivity of all the samples increases with increasing temperature. This behavior could be described by Arrhenius relation [16],

$$\sigma = A\exp\left(\frac{-E_a}{kT}\right) \qquad ...3$$

Where, A is a temperature independent constant, k the Boltzmann constant, E_a the activation energy and T the absolute temperature.

There are three linear regions in different temperature ranges. Calculated values of activation energies are given in Table 3.

Table 3: Activation energies in ferri and para magnetic regions and transition temperatures before and after irradiation.

Activation energy					
Un-irradiated		**300kGy**		**500kGy**	
E_P	E_F	E_P	E_F	E_P	E_F
1.611	0.578	1.203	0.157	1.080	0.088
Transition temperatures (in K)					
430		419		389	

The electrical conduction in region (I) is attributed to the presence of impurities [17, 18]. Impurities are due to the oxygen loss during the sintering process leading to the formation of Fe^{2+} from Fe^{3+} ions for charge balancing. These Fe^{2+} ions act as donor centers [19].

It is observed that the transition temperature decreases upon irradiation [20]. The activation energies in the paramagnetic region E_p (region III)) are greater than that of ferrimagnetic ones E_f (region II)) for all the samples. This increase in activation energy due to magnetic transition is explained as follows: According to Goodenough, 1973 [21], the magnetic transition can be considered as second order, which is characterized by a large temperature range. An increase in the jumping length between the ions causes increase in activation energy. The values of activation energy decreased after irradiation in every region. The reason for this is, due to generation of some vacancies at different depths, acting as trapping centers causing a decrease of the jumping length of charge carriers [22].

4. Conclusions

The crystallite size decreases and lattice strain increases with dose, due to creation of lattice vacancies resulting in structure distortion.

D C electrical conductivity of the irradiated samples at room temperature is increased due to the increase of ratio Fe^{2+}/Fe^{3+}.

The activation energy decreases after irradiation due to generation of some vacancies at different depths.

5. Acknowledgements

The authors wish to thank Dr. H M Somashekarappa, Head, Centre for Application of Radioisotopes and Radiation Technology (CARRT), Mangalore University and Prof. R Somashekar, Center for Materials Science, Vijnana Bhavan, University of Mysore, Manasagangotri Campus, Mysore - 570006.

6. References

1. Tianshu Z, Hing P, Jiancheng Z, Lingbing K. Mater. Chem. Phys., 1999; 3(6):192-198.
2. Harish KN. Arch. Appl. Sci. Res., 2013; 5(2):42-51.
3. Ateia E, Egypt J. Solids, 2006; (29):2,
4. Karim A. Nuclear Instruments and Methods in Physics Research B 2010; 268:2706-2711.
5. Angadi B, Jali VM, Lagare MT, Kini NS, Umarji AM, Kumar R *et al*. Nucl. Instrum. Meth. B 2002; 187:87.
6. Deepthy A, Rao KSRK, Bhat HL, Kumar R, Asokan K. J Appl. Phys. 2001; 89:65-60.
7. Ogale SB, Ghosh K, Gu JY, Shreekal R, Shinde SR, Downes MM *et al*. J Appl. Phys. 1998; 84:6255.
8. Bathe R, Date SK, Shinde SR, Saraf LV, Ogale SB, Patil SI *et al*. J Appl. Phys. 1998; 83:7174.
9. Minal A. Taiwade Der Pharma Chemica, 2013; 5(5):301-306
10. Miyata N. J Phys. Soc. Japan, 1961; 16:206.
11. Sattar AA, El-Sayed HM, El-Shokrofy KM, El-Tabey MM. J App. Sci., 2005; 5:162.
12. Mason TO, Bowen HK. J Am. Ceram. Soc., 1981; 64:237.
13. Hemeda M, El-Saadawy M. J Magn. Magn. Mater. 2003; 256:63.
14. Dalal Mohammed Hemeda. J Appl. Sci. 2005; 2(5):989.
15. Hamada IM. J Magn. Magn. Mater. 2004; 271:318.
16. Sattar AA, El-Sayed HM, El-Shokrofy KM, Eltabey MM. J Mater. Sci., 2007; 42:149-155. DOI 10.1007/s10853-006-1087-3.
17. Ravinder D. Mat. Lett., 2000; 45:68-70. DOI: 10.1016/S0167-577X(00)00078-1
18. Sattar AA, El-Sayed HM, Eltabey MM. J Mater. Sci., 2005; 40:4873-4873. DOI: 10.1007/s10853-005-3884-5.
19. Bhise BV, Lotke SD, Patil SA. Phys. Stat. Sol., 1996; 157:411-419. DOI: 10.1002/pssa.2211570225.
20. Mohamed Eltabey, American Journal of Applied Sciences 2014; 11(1):109-118,
21. Goodenough JB. Mater. Res. Bull., 1973; 8:423-431. DOI: 10.1016/0025-5408(73)90046-9.
22. Ahmed MA, Ateia E, Abdelatif G, Salem FM. Mater. Chem. Phys., 2003; 81:63-77. DOI:10.1016/S0254-0584(03)00143-3.